Non-invasive Imaging and Tracking of Engineered Human Muscle Precursor Cells for Skeletal Muscle Tissue Engineering Using Positron Emission Tomography

Deana Haralampieva[1,2,3], Thomas Betzel[1], Ivana Dinulovic[4], Souzan Salemi[2], Meline Stoelting[2], Stefanie Kraemer[1], Roger Schibli[1], Tullio Sulser[2], Christoph Handschin[4], Daniel Eberli[2,3], Simon M. Ametamey[1,3]

[1]ETH Zurich, Institute of Pharmaceutical Sciences, Vladimir-Prelog-Weg 4 CH-8093 Zurich, Switzerland
[2]University Hospital Zurich and University of Zurich, Laboratory for Tissue Engineering and Stem Cell Therapy, Department of Urology, Frauenklinikstrasse 10, CH-8091 Zurich, Switzerland
[3]Zurich Center for Integrative Human Physiology (ZIHP)
[4]Biozentrum, Focal Area Growth and Development, University of Basel, Klingelbergstrasse 50-70, CH-4056 Basel, Switzerland

This research was originally published in J Nucl Med. 2016 57(9):1467-73. PMID: 27199355. doi: 10.2967/jnumed.115.170548

Reprint request

Unfortunately, due to copyright-relatedt issues, we are not able to post the post-print pdf version of our manuscript - in some cases, not even any version of our manuscript. Thus, if you would like to request a post-production, publisher pdf reprint, please click send an email with the request to christoph-dot-handschin_at_unibas-dot-ch (see http://www.biozentrum.unibas.ch/handschin).

Information about the Open Access policy of different publishers/journals can be found on the SHERPA/ROMEO webpage: http://www.sherpa.ac.uk/romeo/

Reprint Anfragen

Aufgrund fehlender Copyright-Rechte ist es leider nicht möglich, dieses Manuskript in der finalen Version, z.T. sogar in irgendeiner Form frei zugänglich zu machen. Anfragen für Reprints per Email an christoph-dot-handschin_at_unibas-dot-ch (s. http://www.biozentrum.unibas.ch/handschin).

Informationen zur Open Access Handhabung verschiedener Verlage/Journals sind auf der SHERPA/ROMEO Webpage verfügbar: http://www.sherpa.ac.uk/romeo/

Non-invasive Imaging and Tracking of Engineered Human Muscle Precursor Cells for Skeletal Muscle Tissue Engineering Using Positron Emission Tomography

Deana Haralampieva[1,2,3], Thomas Betzel[1], Ivana Dinulovic[4], Souzan Salemi[2], Meline Stoelting[2], Stefanie Kraemer[1], Roger Schibli[1], Tullio Sulser[2], Christoph Handschin[4], Daniel Eberli[2,3], Simon M. Ametamey[1,3]

[1]ETH Zurich, Institute of Pharmaceutical Sciences, Vladimir-Prelog-Weg 4 CH-8093 Zurich, Switzerland
[2]University Hospital Zurich and University of Zurich, Laboratory for Tissue Engineering and Stem Cell Therapy, Department of Urology, Frauenklinikstrasse 10, CH-8091 Zurich, Switzerland
[3]Zurich Center for Integrative Human Physiology (ZIHP)
[4]Biozentrum, Focal Area Growth and Development, University of Basel, Klingelbergstrasse 50-70, CH-4056 Basel, Switzerland

Running Title: Imaging of Engineered Human MPCs

*__corresponding author__
Simon M. Ametamey, PhD
Institute of Pharmaceutical Sciences, ETH Zurich
Vladimir-Prelog-Weg 4
8093-Zurich, Switzerland
Tel:+41446337463
Fax:+41446331367
E-Mail: simon.ametamey@pharma.ethz.ch

*__first author__:
Deana Haralampieva, MSc, PhD student
University Hospital Zurich and ETHZ
Department of Urology
Laboratory for Tissue Engineering and Stem Cell Therapy
Frauenklinikstrasse 10
8091-Zurich, Switzerland
Tel:+41(0)795788654
Fax:+41442556004
E-Mail: deana.haralampieva@usz.ch

Word count:4988

Financial support: this work was supported by the Swiss National Science Foundation (SNF,CRSII3_136197/1), Promedica and Novartis Foundation for Medical-Biological Research.

ABSTRACT:
Transplantation of human muscle precursor cells (hMPCs) is envisioned for the treatment of various muscle diseases. However, a feasible non-invasive tool to monitor cell survival, migration and integration into the host tissue is still missing. **Methods**: In this study, we designed an adenoviral delivery system to genetically modify hMPCs to express a signaling-deficient form of a human dopamine D2 receptor (hD2R). The gene expression levels of the receptor were evaluated by Reverse Transcriptase Polymerase Chain Reaction (RTPCR) and infection efficiency was visualized by fluorescent microscopy. Viability, proliferation and differentiation capacity of the transduced cells were confirmed and their sustained myogenic phenotype was shown by flow cytometry analysis and fluorescent microscopy. 18F-Fallypride and 18F-FMISO, two well-established PET radioligands, were successfully synthesized and evaluated for their potential to image engineered hMPCs in a mouse model. Furthermore, biodistribution studies and autoradiography were also performed to determine the extent of signal specificity. **Results**: To address the feasibility of the presented approach for tracking of hMPCs in an *in vivo* model, we first evaluated the safety of the adenoviral gene-delivery, which showed no detrimental effects on the primary human cells. Specific binding of 18F-Fallypride to hD2R_hMPCs was demonstrated *in vitro*, as well as *in vivo*, by performing autoradiography, biodistribution and PET experiments, respectively. Furthermore, 18F-FMISO uptake was evaluated at different time-points after cell inoculation *in vivo*, showing high signal only at the early stages. Finally, histological assessment of the harvested tissues confirmed the sustained survival of the transplanted cells at different time-points with formation of muscle tissue at the site of injection. **Conclusion**: We here propose a signaling-deficient human D2R as a potent reporter for *in vivo* hMPCs PET tracking by 18F-Fallypride. This approach is a significant step forward towards a potential non-invasive tracking of hMPC_hD2R cells and bioengineered muscle tissues in the clinic.

Key Words: human muscle precursor cells, dopamine 2 receptor, hypoxia, *in vivo* imaging, PET

INTRODUCTION

To date, organ transplantation is the gold standard for rescuing damaged tissues. This method comes with a number of drawbacks such as dependence on donor organs and the high morbidity of immunosuppressive therapy. Regenerative medicine using autologous stem cells may offer an alternative approach for organ and tissue replacement, overcoming the known pitfalls(1-3). Tissue engineering, a major regenerative medicine component, follows the principles of cell transplantation, materials science, and engineering towards the development of biological substitutes that can restore and maintain normal function(4). Due to their regenerative capacity, MPCs are investigated for skeletal muscle tissue reconstruction and replacement(5). These adult stem cells reside on muscle fibers periphery, where they are activated after injury, proliferating, differentiating into myoblasts and later fusing to form new myofibers, thereby granting sufficient progeny for repetitive tissue repair(6). The majority of MPCs are committed to the myogenic lineage and are therefore the most suitable source for muscle engineering(7). Recent preclinical studies have shown that muscle reconstruction using MPCs is a promising and feasible therapy(8), however, the fate of the cells after implantation still needs to be further investigated.

Currently, these issues are addressed by histological assessment, which has one major shortcoming: the invasiveness of biopsies and bioengineered muscle tissue destruction. Novel non-invasive imaging technologies are therefore needed. Molecular imaging is an emerging field, providing essential information about heterogeneous human disorders. While bioluminescence has very poor spatial resolution and magnetic resonance imaging lacks the high sensitivity of radionuclide-based tools, PET/CT is a system with both high resolution and high sensitivity(9). Although imaging reporter genes are available for fluorescence, bioluminescence and magnetic resonance imaging, only radionuclide-based reporter genes are currently investigated for use in patients(10-12). One such system is based on the D2R imaging using PET. Natively, the D2R expression is largely limited to the striata nigra brain region(13). A large number of specific and high-affinity D2R PET ligands are available, some of which have found routine application in the clinic(14). Thus, the PET imaging of exogenously added hD2R in cells injected in peripheral body regions would be an attractive method to track the hD2R *in vivo*. One potential shortcoming of this approach, however, is the possible induction of undesired biological effects by gene introduction and by alteration of intracellular signalling pathways. As binding of the D2R ligand would activate Gprotein-linked signalling pathway, a mutated rat receptor (D2R80A) has been reported, that uncouples ligand binding from intracellular signal transduction(15),(16). However, there are limits to the amount of signal production, as one receptor interacts with only one ligand molecule and can potentially be blocked by non-labelled endogenous ligands(17).

Skeletal muscle cells are a key target for many stem cell and gene therapy applications. With PET imaging gaining increasing importance in regenerative medicine, it is of high interest to study transfected MPCs as cell types that could be used to restore muscle function. In this study, we investigated the possibility of using PET/CT imaging to non-invasively monitor implanted and genetically modified hMPCs_hD2R in a mouse model. Specifically, our main aim was to study the location, level of expression and survival duration of the engineered hMPCs

using hD2R as a reporter gene. The accomplishment of this goal would help to improve our understanding of the behaviour of hMPCs during *in vivo* differentiation.

MATERIALS AND METHODS

Isolation and Expansion of hMPCs

Human muscle biopsies from *Musculus rectus abdominis* were randomly collected after approval by the local institutional review board and after written informed consent of hospitalized patients undergoing abdominal surgery. All samples were processed according to established protocols(18).

Adenoviral Design

The AdEasy System (Stratagene(19)) was used for recombinant adenovirus construction. Briefly, we mutated phenylalanine 411 of the hD2R into alanine (F411A) to obtain a signalling-deficient hD2R that still binds ligands in a normal manner but will not activate intracellular signalling upon ligand binding(20). In detail, IRAUp969E0451D vector containing hD2R (ImaGenes) and pcDNA3 plasmid containing monomer red fluorescent protein (m)RFP (Addgene) were purchased. The hD2R was subcloned into the pcDNA3.1 TOPO expressional vector (Invitrogen), which resulted in addition of C-terminal 6xHis and V5 tags. Next, the F411A point-mutation was introduced by site-directed-mutagenesis (Stratagene). The hD2R and mRFP sequences were then subcloned into the backbone of the pShuttle-cytomegalovirus vector (Addgene), ensuring a robust, constitutive expression. The final vector thus contained hD2R and RFP sequences, both running under two separate cytomegalovirus promoters. Successful cloning was validated by sequencing, while viral infection and gene expression were monitored by visualizing RFP and RTPCR, respectively. The transduced cells were expanded for 2 days after infection and were subcutaneously (*s.c.*) injected into nude mice.

Cell Viability and Proliferation

In all cases, cell numbers and viability were confirmed by trypan blue staining. To evaluate proliferation and viability of the infected cells at different time points, hMPCs were cultured for 6 days. The cell proliferation reagent WST-1 (Roche) was used according to manufacturer's protocol. For further confirmation of cell viability, hMPCs were stained with 10 µM CellTrace Calcein green, AM (Life Technologies), 30min, 37 °C. Viable cells were detected using a fluorescence microscope. All measurements were repeated at least three times and samples were analyzed in triplicates.

Radiosynthesis of 18F-Fallypride

The synthesis of 18F-Fallypride was accomplished in a one-step reaction according to a published procedure(21). The radiotracer was obtained in radiochemical purity >95% and specific activity ranged from 32-168 GBq/µmol.

Radiosynthesis of 18F-FMISO

18F-FMISO was obtained in a two-step reaction in analogy to a previously published method(22). The final formulated product was obtained in a decay corrected radiochemical yield ranging from 25-37%. Radiochemical purity was >95% and specific activities ranged from 34-190GBq/µmol.

In vitro 18F-Fallypride Uptake assay
The experiment was performed in longitudinally truncated 24-well-plates testing two AV-hD2R constructs in three concentrations (500ng, 1µg, 2µg/well). Approximately 20`000 hMPCs/well were seeded and after 24h the cells were infected with the corresponding constructs for 2 days. The modified cells were incubated with 18F-Fallypride [1nM] for 15 min and scanned 26 min after start of incubation. The cells were imaged using small animal PET scanner. The scan duration was 45 min. All experiments were performed in triplicates.

Animal Experimentation
All animal experiments were approved by the local animal care committee. A total of 46 female, 8 week old nude mice (Charles River) were used for this study. The hMPCs were expanded to passage 3-4 for the *in vivo* experiments. Each sample contained $30x10_6$ transduced hMPCs, which were gently mixed with 500µL collagen type I carrier (final concentration: 2mg/mL) (BD) and prepared for *s.c.* injection in the back of nude mice(23). Each animal received two bilateral s.c. injections (including control-collagen only injections). The engineered skeletal muscle tissues were harvested after 1, 2, and 4 weeks.

Tracking of Bioengineered Muscle Tissues via PET/CT Imaging
PET experiments were performed with a dedicated small animal PET/CT tomograph eXplore VISTA (General Electric), which uses the phoswich detector technology in a dual ring set-up(24). For 18F-Fallypride administration, mice were restrained and injected via a lateral tail vein with 4.38-26.25MBq (0.17-2.34nmol) of the radioligand. For blockage experiments, Haloperidol (1mg/kg) was injected. Ten minutes after radiotracer injection, animals were anesthetized with isoflurane in air/oxygen mixture, positioned and fixed on the bed of the camera. PET data were acquired to yield dynamic images with sufficient count statistics. Depth of anesthesia and body temperature were monitored and controlled according to a previously published protocol(25). In addition, respiratory frequency was controlled with 1025T monitoring system from SA Instruments (Stony Brook, NY). After the PET scan, animals recovered from anesthesia and were rescanned at a later time point with the next tracer. Raw data were reconstructed by 2D-OSEM algorithm and the obtained image data were evaluated by visual inspection and semiquantitative volume-of-interest(26) analysis using the dedicated software PMOD.

Biodistribution Studies
The subsequent post-mortem biodistribution assessment was performed 60 min post i.v. injection of 18F-Fallypride. Tracer uptake in engineered muscle tissue, striatum nigra, native muscle tissue, cerebellum and injected collagen was evaluated in a gamma-counter (CobraIIAuto-gamma, Canberra Packard, Groningen, Netherlands).

Autoradiography
Cryosections (20µm) of frozen samples were pre-incubated on ice for 12min in TRIS/HCl, 0.1% BSA, pH 7.4. Then, the slides were incubated with 18F-Fallypride [0.03nM] in the presence and absence of Haloperidol [10µM] as blocker for 60min. After air-drying the tissue slices were exposed to phosphorimager plates which

were analysed with Fuji BAS-5000 phosphorimager.

Histological Assessment

The harvested engineered muscle tissues were embedded in cryo-preservative (OCT embedding medium, Cell Path) immediately after isolation. Cryosections were prepared (10μm) and further processed. Haematoxylin and eosin (H&E) (Sigma) staining was performed according to the manufacturer's protocol.

Statistics

For statistical analysis IBM SPSS v22.0 (SPSS Inc,) was used and graphs were drawn with GraphPad Prism v5.04 (GraphPad Software, Inc.). All data were analysed by Student's *t*-tests or one-way ANOVA with Bonferroni or LSD post-hoc analysis ($p<0.05$ was considered significant). All presented data are expressed as means with corresponding standard error of the mean (±SEM).

RESULTS

Viability, Proliferation and Differentiation Rates of Genetically Modified hMPC_hD2R

The adenoviral construct containing hD2R (F411A) was generated and amplified for further use in hMPCs. Non-toxicity of the viral infection was visualized by a cell viability assay (calcein) (Fig.1A, green), where no significant differences between WT and hD2R-infected cells were detected. The transduction efficiency of ~25% infected cells was confirmed by fluorescent imaging, as the designed construct contained a red fluorophore, expressed under a separate cytomegalovirus promoter (Fig.1A, red). This construct allowed assessment of cell transduction efficiency prior to transplantation. Using a fiber formation assay(27), we evaluated the capability of hMPCs to form myofibers *in vitro* (Fig.1A, third row). Comparison between WT and hD2R-overexpressing cells (Supplemental Fig.1) did not reveal any significant difference in the number of nuclei per fiber (p=0.8629, WT: 8.325±0.6818, n=83; hD2R: 8.184±0.4635, n=87), number of nuclei per highpower-field (WT: 230.6±14.34, n=10; hD2R: 216.9±10.71, n=10, p=0.4539) and the number of fibers per high-power-field (WT: 8.3±0.8699, n=10; hD2R: 8.4±0.5812, n=10, p=0.9249). The calculated overall fusion did not differ between infected and WT cells either (WT: 30.95±3.289, n=10; hD2R: 32.40±3.085, n=10, p=0.7512). Successful transduction was also confirmed by hD2R gene expression levels (Fig.1B, n=3x3, p=0.005). Furthermore, proliferation capacity of the WT and hD2Roverexpressing
hMPCs was determined by cell proliferation assay over 3 days culturing following transduction, showing no significant variations between the different groups (Fig.1C, WT: 2.2173±0.364, n=6; hD2R: 2.0843±0314, n=6, p=0.787 at 3 days).

Flow Cytometry and Immunocytochemistry Analysis of hMPC_hD2R

Initially, the cells were analyzed by flow cytometry (Fig.2A), and in parallel by immunocytochemistry (Fig.2B) 2 days after infection, revealing a sustained muscle phenotype without significant alterations between the groups.

In Vitro PET/CT Imaging of hMPC_hD2R Using 18F-Fallypride

Before each experiment, the infection efficiency was assessed by fluorescent microscopy and positive cells were further processed for *in vitro* or *in vivo* studies. Initially, the capacity of the transduced hMPCs_hD2R to efficiently bind 18FFallypride was evaluated *in vitro*. When using the designed adenovirus, testing 3 different concentrations of viral particles for tracer uptake, we observed a high binding affinity (Fig.3A). As expected, the cells infected with the highest non-toxic concentration showed the highest detectable PET signal (first row, 10x) and were thus used for further experiments. These data confirm the efficiency of the presented hD2R adenoviral construct for hMPCs genetic modification.

In Vivo PET/CT Imaging of hMPC_hD2R Using 18F-Fallypride

Encouraged by our *in vitro* results, we evaluated the capability of transduced hMPCs to specifically bind 18F-Fallypride in an established *ex situ* model for skeletal muscle tissue formation *in vivo*. The hMPC_hD2R showed high

standardized uptake value (SUV) after 1 week (SUV: 0.259±0.019, n=8). This signal decreased after two weeks (SUV: 0.169±0.019, n=8, p=0.005) and no significant difference to background was observed after 4 weeks (SUV: 0.134±0.014, n=6, p<0.0001) (Fig.3B). Animals injected with collagen only did not show a significant radiotracer accumulation at any time (SUV: 0.115±0.011, n=10). Cerebellum brain region was used as negative control, showing negligible nonspecific uptake (SUV: 0.124±0.006, n=16). This was confirmed by VOI (26) analysis, where significantly higher signal-to-background ratio of at least 2.08 at the earliest time point was observed (Fig.3B). Biodistribution assessment also showed significant decrease in tracer uptake in engineered tissues over time (Fig.4A, n=4-16 per time point). Signal specificity was demonstrated in *in vivo* PET studies using haloperidol as D2R blocking agent; the striatum region was visualized as positive control (Fig.4B). Additionally, radioligand binding specificity was demonstrated in autoradiography studies, whereby hD2R-expressing tissues (including native controls) showed reduction of radioligand uptake after incubation with haloperidol (Fig.4C), confirming the *in vivo* data.

PET Imaging of Hypoxia Using 18F-FMISO during Formation of Bioengineered Skeletal Muscle Tissue

After successful tracking of the injected hMPC_hD2R, we were further interested in studying the oxygenation status of the cells after implantation. To address this we utilized 18F-FMISO, a PET radiotracer for visualizing hypoxic regions. One week after cell inoculation, a relatively high 18F-FMISO uptake was observed which decreased at later time points (Fig.5A). VOI analysis of the first week samples (SUV: 0.315±0.02, n=8) showed a mean signal change ratio of 1.6, compared to later time points (2wk: SUV: 0.189±0.019, n=8; 4wk: SUV: 0.205±0.009, n=6) and negative controls (cerebellum: SUV: 0.206±0.017, n=16; collagen: SUV: 0.251±0.003, n=10 (Fig.5B)).

Histological Assessment, Gene and Protein Analysis of the Harvested Tissues

The relative protein expression of typical skeletal muscle protein markers (sarcomeric α-actinin, MyHC), vWf and hD2R were evaluated after tissue harvest by Western Blot (Fig.6A). *Tibialis anterior* (TA) and *striatum nigra* (SN) were used as controls. The protein expression levels of sarcomeric markers gradually increased in the bioengineered tissue samples (MyHC: 0.4211±0.033, n=4 (1wk); 2.1915±0.407, n=6 (2wk); 3.0734±0.72, n=8 (4wk), p=0.012, respectively; α-actinin: 0.4065±0.111, n=4 (1wk); 0.6734±0.113, n=6 (2wk); 1.2696±0.315, n=8 (4wk), p=0.043, respectively), corresponding to the expected timeline of muscle fiber formation (Fig.6A). The relative hD2R protein expression decreased steadily over time (2.4072±0.608, n=3 (1wk); 1.5881±0.25, n=6 (2wk); 1.0394±0.294, n=12 (4wk), p=0.031, respectively) (Fig.6A), concomitant with the observed decrease of 18F-Fallypride uptake (Fig.3B). The decrease in 18F-FMISO uptake over time coincided with an increase in vWf protein levels (endothelial cell marker, n=4) (Fig.6A), as well as with a rising vascular endothelial growth factor (VEGF-A) gene expression (Supplemetal Fig.2B, n=9) in the bioengineered muscle tissues. Although hD2R protein levels were decreasing over time, the corresponding gene expression levels were increasing (Supplemental Fig.2B). The gradual decrease in

size due to collagen remodeling and myofiber formation has previously been reported(23) (Supplemental Fig.2A). Histological analysis revealed successful myofiber formation in the harvested tissues and could illustrate the individual cells of the samples at week 1 and the myotube formation at week 2 and 4 (Fig.6B).

DISCUSSION

Transplantation of MPCs has been considered as a treatment option for genetic and acquired muscle disorders(23, 28) and provides a prospect to reestablish damaged muscle function in patients with muscle degeneration(29). Various research groups demonstrated the formation of muscle tissue after cellular inoculation(30). However, the long-term non-invasive tracking of bioengineered muscle tissue has not been addressed so far.

The need to develop a system combining the use of well-established PET probes and the engineering of a novel vector for expression of the hD2R in hMPCs has prompted our research towards non-invasive visualization of a cell therapy for application in skeletal muscle bioengineering. The generation of a vector coding for a signaling-deficient hD2R was an important milestone as redundant cell-signaling is a major issue in gene therapies.

In this study, we describe a method for metabolic imaging and tracking of hMPCs using PET/CT, thereby illustrating their exact position and the oxygenation state of the newly formed skeletal muscle tissue over time. The results of our studies indicated that: 1) the signaling-deficient hD2R could be efficiently introduced into primary hMPCs, 2) no detrimental effects on cell viability and differentiation were detected, 3) myogenic marker gene expression was unaltered, 4) the receptor was traceable with high specificity using 18F-Fallypride both in cells *in vitro* as well as after injection *in vivo* and 5) receptor expression in the engineered tissues could be validated by autoradiography. We found that the capacity to track the hD2R_hMPCs is excellent in the first week and declines later on. Interestingly, while mRNA expression of hD2R remained high, its protein levels steadily declined. This indicates that the ectopically expressed hD2R is either post translationally modified and/or internalized upon constitutive expression and ultimately degraded during the process of final differentiation to myofibers. Our data showed that by using a high-affinity PET ligand and a mutated hD2R we were able to provide important information on localization, survival and metabolic features for the early phase after cell injection.

A general problem in tissue engineering approaches is the increased oxygen demand and lack of initial vascularization during the early phases of tissue formation, leading to central necrosis(31). Any engineered tissue larger than 0.3 cm^3 requires rapid vascularization to guarantee survival of cells located within the core of the construct. Vascularization of bioengineered tissue is therefore a bottleneck. Hypoxia, which is inversely proportional to the degree of vascularization can be analysed by invasive and non-invasive methods in tissues. The oxygenation status of cells and tissues can be determined by invasive pO2-measurements using polarographic needle electrodes or with fiber-optic probes(32-34). Noninvasive methods include the use of bio-reductive chemical markers, such as 2-nitroimidazoles(35). They form adducts under hypoxic conditions and are irreversibly bound in hypoxic cells. 18F-FMISO is the most widely used PET radioligand for imaging hypoxia in humans(36-38).

In our study with 18F-FMISO, we detected metabolically active bioengineered tissues with low oxygen levels, i.e. where reductive reactions dominate due to low oxygen supply or high oxygen consumption, typical for the early stages of cell-to-myofiber formation. It has been shown that the level of

oxygenation is influenced by the degree of vascularization and by the metabolic consumption of oxygen by engineered tissue(39). Concomitant with our *in vivo* observations, increased VEGF release in a hypoxic environment has been shown to lead to enhanced differentiation(40). Histological analysis confirmed the cell-tomyofiber
transition, correlating with normalized vascularization levels. In line with these observations, using 18F-FMISO for hypoxia imaging of bioengineered constructs seems to be a feasible method.

CONCLUSION

Knowledge of the fate of the inoculated primary hMPCs is a prerequisite for future clinical implementation of this cell therapy. Combining the recent developments in designing robust vectors and novel highly-specific PET imaging probes, we were able to offer an elegant solution, obviating the need for a destructive tissue biopsy. Our study marks a significant step forward towards the non-invasive tracking of hMPC_hD2R cells and bioengineered muscle tissues in the clinic using PET.

Disclosure

The authors recognize the research efforts of those who have contributed to this field of study and declare no conflict of interest.

ACKNOWLEDGEMENTS

Special thanks to Damina Balmer for the critical assessment of this manuscript and Claudia Keller for the technical assistance with the PET/CT scanner.

REFERENCES

1. Chun SY, Cho DH, Chae SY, et al. Human amniotic fluid stem cell-derived muscle progenitor cell therapy for stress urinary incontinence. *J Korean Med Sci.* 2012;27:1300-1307.
2. Nikolavasky D, Stangel-Wojcikiewicz K, Stec M, et al. Stem cell therapy: a future treatment of stress urinary incontinence. *Semin Reprod Med.* 2011;29:61-70.
3. Aref-Adib M, Lamb BW, Lee HB, et al. Stem cell therapy for stress urinary incontinence: a systematic review in human subjects. *Arch Gynecol Obstet.* 2013;288:1213-1221.
4. Olson JL, Atala A, Yoo JJ. Tissue engineering: current strategies and future directions. *Chonnam Med J.* 2011;47:1-13.
5. Smaldone MC, Chancellor MB. Muscle derived stem cell therapy for stress urinary incontinence. *World J Urol.* 2008;26:327-332.
6. Hill M, Wernig A, Goldspink G. Muscle satellite (stem) cell activation during local tissue injury and repair. *J Anat.* 2003;203:89-99.
7. Benchaouir R, Rameau P, Decraene C, et al. Evidence for a resident subset of cells with SP phenotype in the C2C12 myogenic line: a tool to explore muscle stem cell biology. *ExpCell Res.* 2004;294:254-268.
8. Eberli D, Aboushwareb T, Soker S, et al. Muscle precursor cells for the restoration of irreversibly damaged sphincter function. *Cell Transplant.* 2012;21:2089-2098.
9. Deana G. Haralampieva SMA, Tullio Sulser, Daniel Eberli. Non-invasive imaging modalities for clinical investigation in regenerative medicine *Cells and Biomaterials in Regenerative Medicine*: InTech; 2014:175-197.
10. Penuelas I, Mazzolini G, Boan JF, et al. Positron emission tomography imaging of adenoviral-mediated transgene expression in liver cancer patients. *Gastroenterology.* 2005;128:1787-1795.
11. Penuelas I, Haberkorn U, Yaghoubi S, et al. Gene therapy imaging in patients for oncological applications. *Eur J Nucl Med Mol Imaging.* 2005;32 Suppl 2:S384-S403.
12. Dempsey MF, Wyper D, Owens J, et al. Assessment of 123I-FIAU imaging of herpes simplex viral gene expression in the treatment of glioma. *Nucl Med Commun.* 2006;27:611-617.
13. MacLaren DC, Gambhir SS, Satyamurthy N, et al. Repetitive, non-invasive imaging of the dopamine D2 receptor as a reporter gene in living animals. *Gene Ther.* 1999;6:785-791.
14. Siessmeier T, Zhou Y, Buchholz HG, et al. Parametric mapping of binding in human brain of D2 receptor ligands of different affinities. *J Nucl Med.* 2005;46:964-972.
15. Liang Q, Satyamurthy N, Barrio JR, et al. Noninvasive, quantitative imaging in living animals of a mutant dopamine D2 receptor reporter gene in which ligand binding is uncoupled from signal transduction. *Gene Ther.* 2001;8:1490-1498.
16. Schonitzer V, Haasters F, Kasbauer S, et al. In vivo mesenchymal stem cell tracking with PET using the dopamine type 2 receptor and 18F-Fallypride. *J Nucl Med.* 2014;55:1342-1347.

21
17. Rodriguez-Porcel M. In vivo imaging and monitoring of transplanted stem cells:

clinical applications. *Curr Cardiol Rep.* 2010;12:51-58.
18. Eberli D, Soker S, Atala A, et al. Optimization of human skeletal muscle precursor cell culture and myofiber formation in vitro. *Methods.* 2009;47:98-103.
19. Luo J, Deng ZL, Luo X, et al. A protocol for rapid generation of recombinant adenoviruses using the AdEasy system. *Nat Protoc.* 2007;2:1236-1247.
20. Cho W, Taylor LP, Mansour A, et al. Hydrophobic residues of the D2 dopamine receptor are important for binding and signal transduction. *J Neurochem.* 1995;65:2105-2115.
21. Mukherjee J, Yang ZY, Das MK, et al. Fluorinated benzamide neuroleptics--III. Development of (S)-N-[(1-allyl-2-pyrrolidinyl)methyl]-5-(3-[18F]fluoropropyl)-2, 3-dimethoxybenzamide as an improved dopamine D-2 receptor tracer. *Nucl Med Biol.* 1995;22:283-296.
22. Lim JL, Berridge MS. An efficient radiosynthesis of [18F]fluoromisonidazole. *Appl Radiat Isot.* 1993;44:1085-1091.
23. Delo DM, Eberli D, Williams JK, et al. Angiogenic gene modification of skeletal muscle cells to compensate for ageing-induced decline in bioengineered functional muscle tissue. *BJU Int.* 2008;102:878-884.
24. Wang Y, Seidel J, Tsui BM, et al. Performance evaluation of the GE healthcare eXplore VISTA dual-ring small-animal PET scanner. *J Nucl Med.* 2006;47:1891-1900.
25. Honer M, Bruhlmeier M, Missimer J, et al. Dynamic imaging of striatal D2 receptors in mice using quad-HIDAC PET. *J Nucl Med.* 2004;45:464-470.
26. Dube D, Brideau C, Deschenes D, et al. 2-heterosubstituted-3-(4-methylsulfonyl)phenyl-5-trifluoromethyl pyridines as selective and orally active cyclooxygenase-2 inhibitors. *Bioorg Med Chem Lett.* 1999;9:1715-1720.
27. Herzog H, Langen KJ, Weirich C, et al. High resolution BrainPET combined with simultaneous MRI. *Nuklearmedizin.* 2011;50:74-82.
28. Mitchell PO, Pavlath GK. Skeletal muscle atrophy leads to loss and dysfunction of muscle precursor cells. *Am J Physiol Cell Physiol.* 2004;287:C1753-1762.
29. Stölting MN, Hefermehl LJ, Tremp M, et al. The role of donor age and gender in the success of human muscle precursor cell transplantation. *J Tissue Eng Regen Med.* 2014.
30. Putman CT, Sultan KR, Wassmer T, et al. Fiber-type transitions and satellite cell activation in low-frequency-stimulated muscles of young and aging rats. *J Gerontol A Biol Sci Med Sci.* 2001;56:B510-519.
31. Lovett M, Lee K, Edwards A, et al. Vascularization strategies for tissue engineering. *Tissue Eng Part B Rev.* 2009;15:353-370.
32. Hockel M, Schlenger K, Aral B, et al. Association between tumor hypoxia and malignant progression in advanced cancer of the uterine cervix. *Cancer Res.* 1996;56:4509-4515.
33. Nordsmark M, Overgaard M, Overgaard J. Pretreatment oxygenation predicts radiation response in advanced squamous cell carcinoma of the head and neck. *Radiother Oncol.* 1996;41:31-39.

22
34. Nordsmark M, Alsner J, Keller J, et al. Hypoxia in human soft tissue sarcomas: adverse impact on survival and no association with p53 mutations. *Br J Cancer.* 2001;84:1070-1075.

35. Machulla H-J. *Imaging of Hypoxia: Tracer Developments*: Springer-Science+Business Media, B.V.; 1999.
36. Bruehlmeier M, Roelcke U, Schubiger PA, et al. Assessment of hypoxia and perfusion in human brain tumors using PET with 18F-fluoromisonidazole and 15OH2O. *J Nucl Med.* 2004;45:1851-1859.
37. Kawai N, Lin W, Cao WD, et al. Correlation between (1)(8)F-fluoromisonidazole PET and expression of HIF-1alpha and VEGF in newly diagnosed and recurrent malignant gliomas. *Eur J Nucl Med Mol Imaging.* 2014;41:1870-1878.
38. Muzi M, Peterson LM, O'Sullivan JN, et al. 18F-Fluoromisonidazole quantification of hypoxia in human cancer patients using image-derived blood surrogate tissue reference regions. *J Nucl Med.* 2015;56:1223-1228.
39. Phelps EA, Garcia AJ. Update on therapeutic vascularization strategies. *Regen Med.* 2009;4:65-80.
40. Bryan BA, Walshe TE, Mitchell DC, et al. Coordinated vascular endothelial growth factor expression and signaling during skeletal myogenic differentiation. *Mol Biol Cell.* 2008;19:994-1006.

Figure Legends

Figure 1. hD2R adenoviral infection did not show adverse effects on hMPC. The adenoviral transduction of hMPCs with hD2R did not affect the cell viability (A, calcein assay, first row, green). Transduction efficiency was shown by fluorescence microscopy (A, second row, red). The ability to form fibers (27) was also not affected by the virus (A; third row). The hD2R gene expression was evaluated (B). Proliferation rate did not differ between WT non-infected and infected hMPCs (C). All measurements were performed in duplicates from at least 3 different biopsies. (Student's *t*-test, *p<0.05). CaAM: calcein AM; FFA: fiber-formation-assay; RFP: red-fluorescent-protein; WT: wild type

Figure 2. Adenoviral infection with hD2R did not change the well-defined hMPC phenotype. The hMPCs were analyzed by flow cytometry (A). Expression of typical muscle markers (green) in the cells expressing hD2R (red) was further confirmed by immunocytochemistry. Nuclei are shown in blue (B). Scale bar: 25µm. (Student's *t*-test, *p<0.05, n=4 biopsies).

Figure 3. Tracking of hMPCs and engineered muscle tissue via PET/CT using 18F-Fallypride *in vitro* and *in vivo*. 18F-Fallypride uptake in hMPC_hD2R was detected at different adenoviral hD2R transduction levels (A). In vivo PET/CT imaging visualized specific tracer uptake in bioengineered tissues over time and VOI analysis illustrated gradual decrease in signal after 1wk (B, n=6-8). SUV: standardized uptake value, VOI: volume-of-interest.

Figure 4. Specificity of 18F-Fallypride signal. Significant enhancement of 18FFallypride
uptake in engineered hMPC_hD2R tissue, compared to collagen and control muscle was observed in a biodistribution study (A, n=4-16). Tracer specificity was evaluated after blockage experiment with Haloperidol (B). Autoradiography showed specific tracer binding (C, lane 1). Blockage was performed with Haloperidol (lane 2) and mouse muscle and rat brain sections were used as negative and positive controls, respectively. Images were averaged from 60 – 120 min. Arrows indicate hMPCs injection site. (one-way ANOVA with Bonferroni post-hoc analysis, *p<0.05), SUV: standardized uptake value

Figure 5. Hypoxia PET/CT monitoring with 18F-FMISO during formation of bioengineered muscle tissues. The redox state of the forming tissues was illustrated with 18F-FMISO [injected activity: 0.49-5.86nmol, 14.86-35.83MBq] (A) and VOIs signal was calculated for 3 different time points (B). Images were averaged from 90–110 min. Arrows indicate hMPCs injection sites.

Figure 6. Protein expression levels were evaluated by Western Blot (A): vWf, MyHC, sarcomeric α-actinin and hD2R expression changes were visualized graphically. H&E staining revealed increasing fiber formation capacity over time (B). *Tibialis anterior* (TA) was used as a control. Scale bar: 100µm (one-way ANOVA with Bonferroni or LSD post-hoc analysis, *p<0.05)

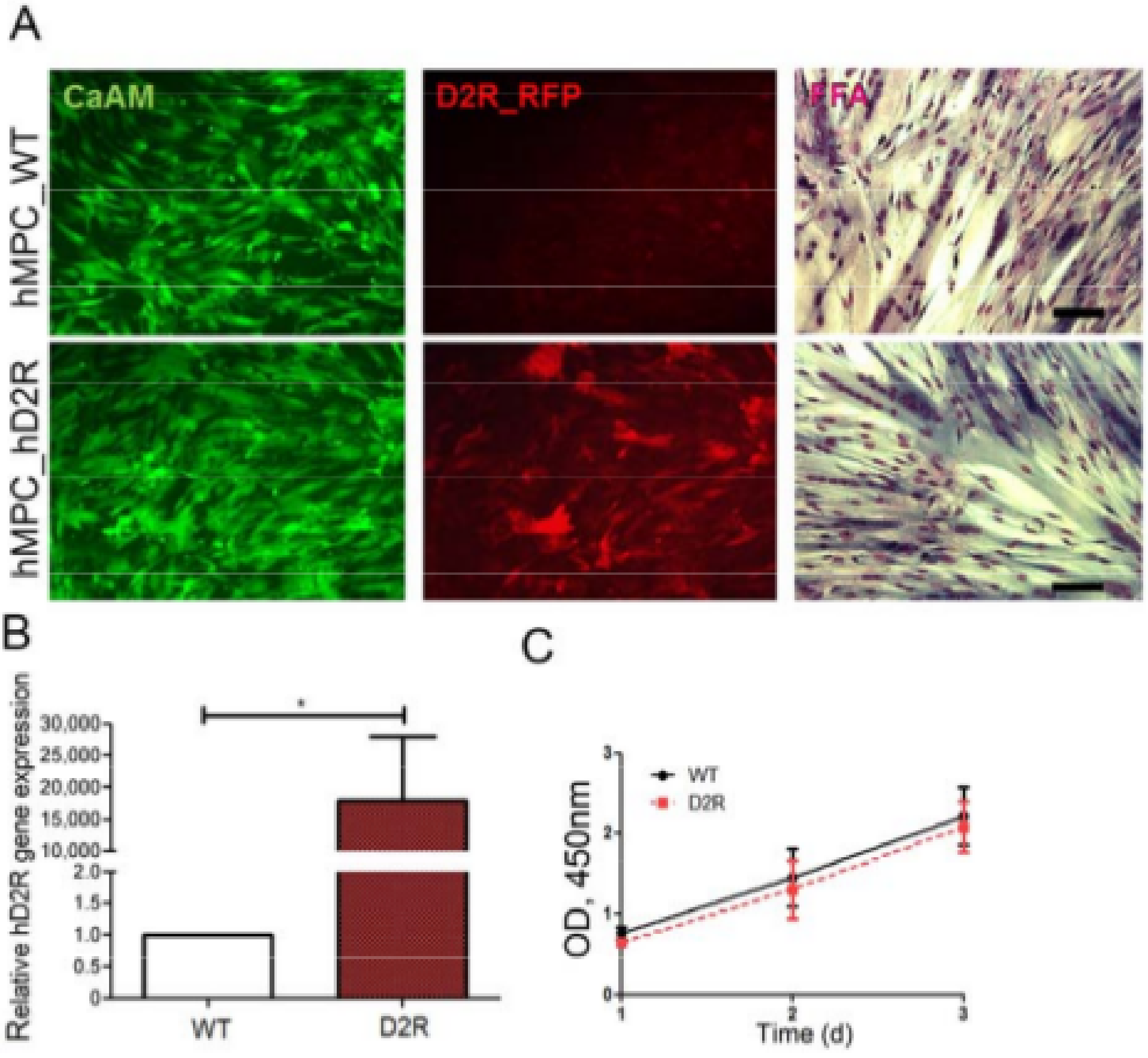
A
CaAM
D2R_RFP
FFA
hMPC_WT
hMPC_hD2R
B
Relative hD2R gene expression
30,000
25,000
20,000
15,000
10,000
2.0
1.5
1.0
0.5
0
WT
D2R
C
OD, 450nm
WT
D2R
Time (d)

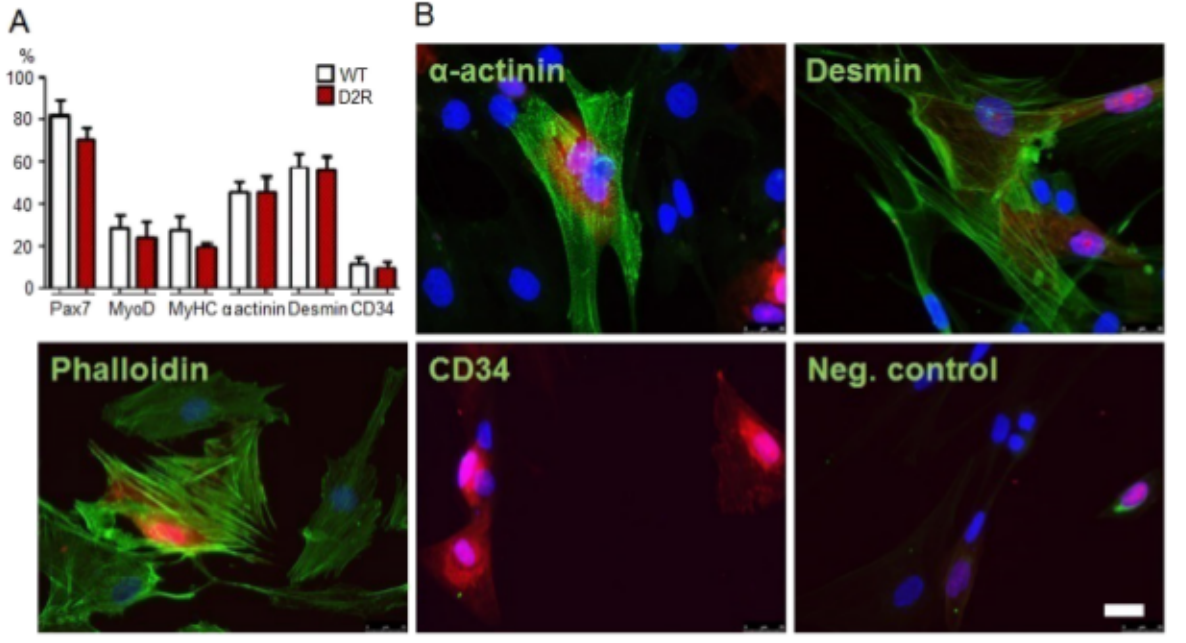
A
%
100
80
60
40
20
0
WT
D2R
Pax7
MyoD
MyHC
α actinin
Desmin
CD34
B
α-actinin
Desmin
Phalloidin
CD34
Neg. control

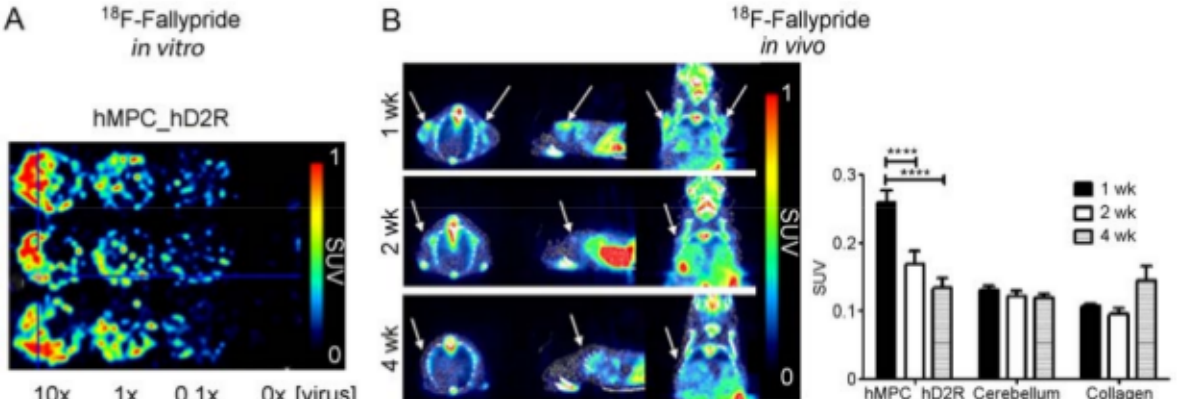
A
^{18}F-Fallypride
in vitro
hMPC_hD2R
1
SUV
0
10x
1x
0.1x
0x [virus]
B
^{18}F-Fallypride
in vivo
1 wk
2 wk
4 wk
1
SUV
0
****
****
0.3
0.2
0.1
0
SUV
1 wk
2 wk
4 wk
hMPC_hD2R
Cerebellum
Collagen

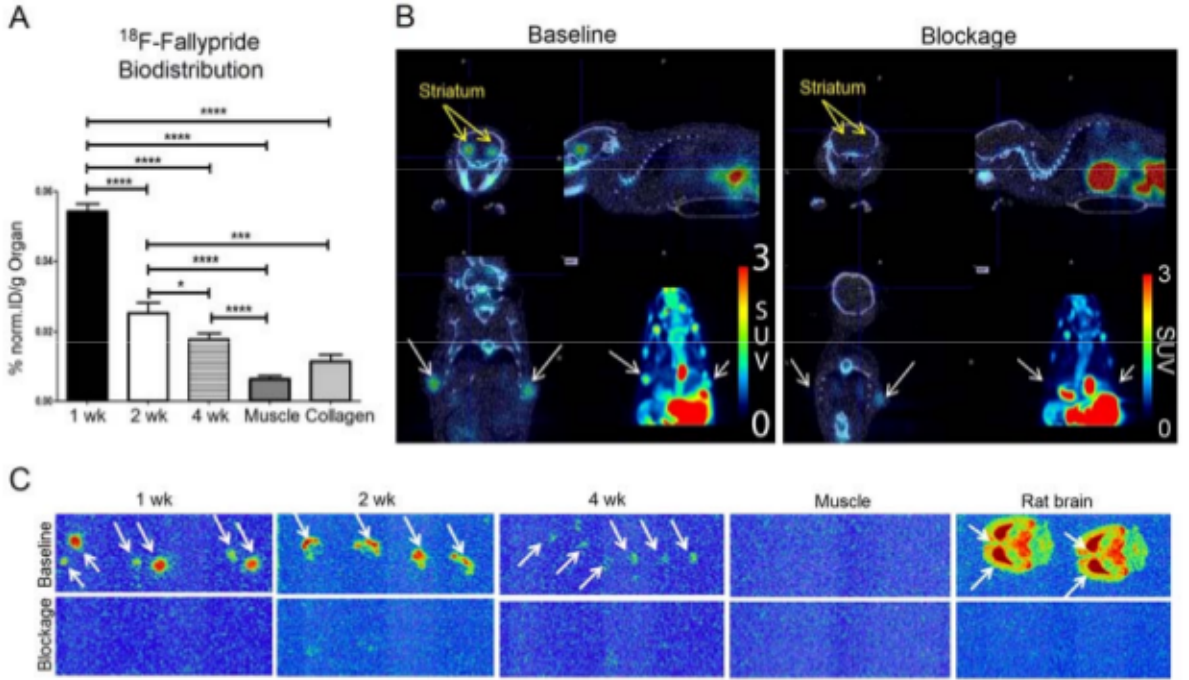
A
18F-Fallypride
Biodistribution
% norm.ID/g Organ
0.06
0.04
0.02
0.00
****
****
****
****
***
****
*
****
1 wk
2 wk
4 wk
Muscle
Collagen
B
Baseline
Blockage
Striatum
Striatum
3
SUV
0
3
SUV
0
C
1 wk
2 wk
4 wk
Muscle
Rat brain
Baseline
Blockage

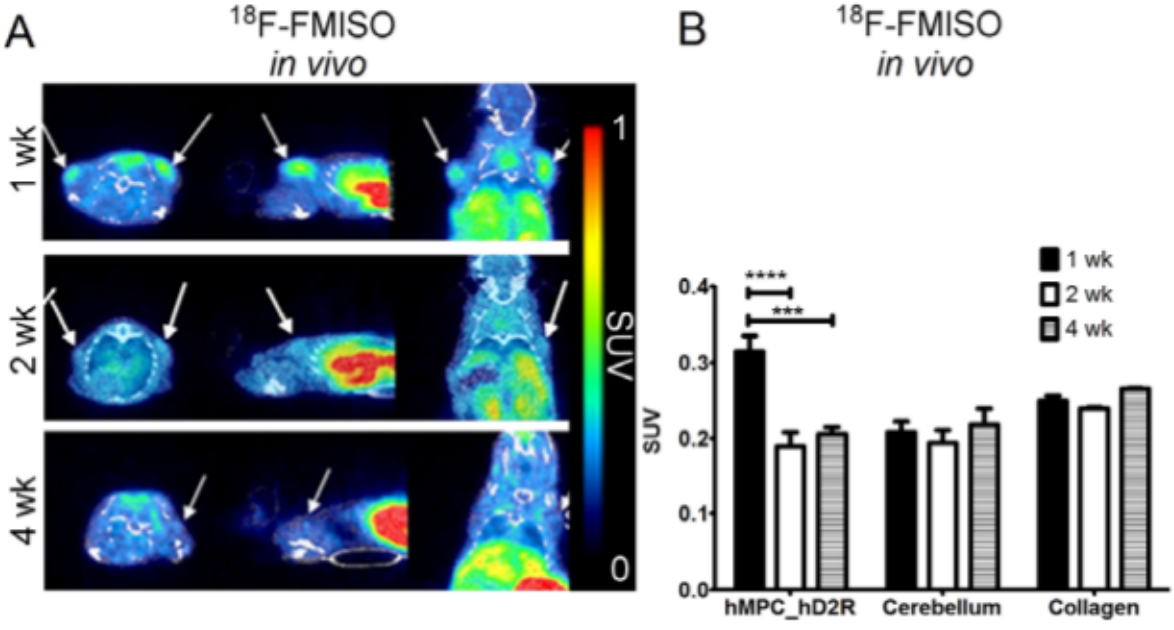
A
18F-FMISO
in vivo
1 wk
2 wk
4 wk
1
SUV
0
B
18F-FMISO
in vivo
1 wk
2 wk
4 wk
****
***
SUV
0.4
0.3
0.2
0.1
0.0
hMPC_hD2R
Cerebellum
Collagen

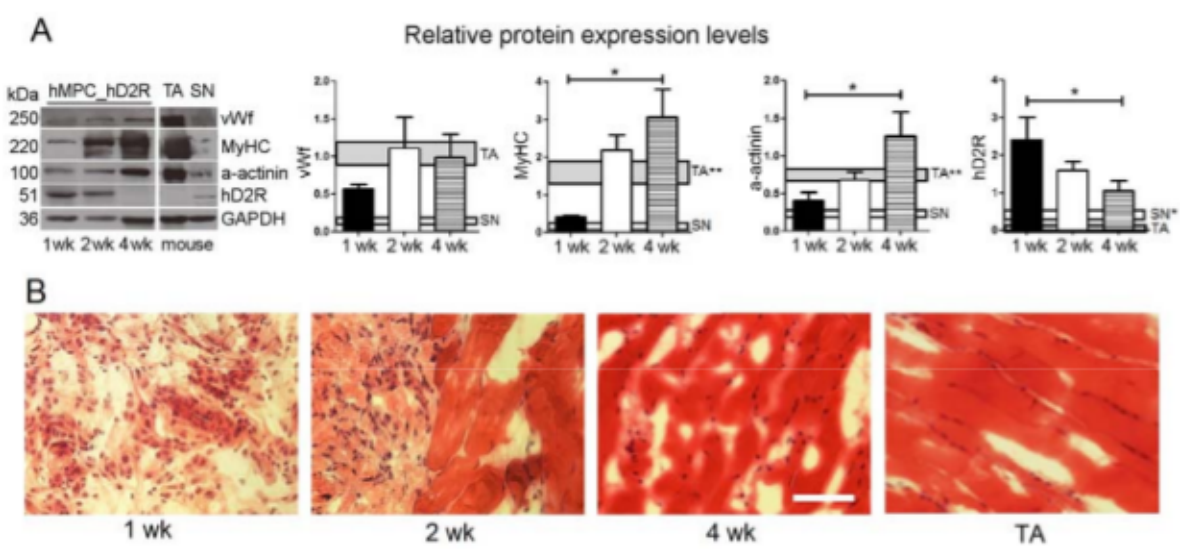
A
Relative protein expression levels
kDa
hMPC_hD2R
TA SN
250
220
100
51
36
vWf
MyHC
a-actinin
hD2R
GAPDH
1wk 2wk 4wk mouse
vWf
MyHC
a-actinin
hD2R
TA
SN
TA**
SN*
1 wk 2 wk 4 wk
B
1 wk
2 wk
4 wk
TA